Research Article

Time-dependent reliability analysis of railway overhead structures

Bin Hu[1] · Ricky W. K. Chan[2]

Abstract

Overhead structures play a vital role in the operation of electrified rail networks. They support overhead electrical wires that provide the necessary power to the operation of trains. Overhead structures are simple steel structures that lack redundancies and failure in a single location may cause significant deformation or complete collapse. Failures of these simple structures have substantial consequences which usually interrupt train service. These steel structures are exposed to the environment and gradual deterioration of steel due to corrosion jeopardizes their strength and serviceability. This paper presents a reliability-based method for strength assessment of portal overhead structures using the first order reliability method. In the resistance formulation, a modified corrosion decay model proposed in this article predicts the thickness loss of wide flange structural steel sections. Meanwhile, load effect formulation follows a structural steel design code and an industry standard. It is found that the bridge-mast connection and the attachment point to drop vertical on the bridge are the most critical parts during the service life of the structure. The reliability analysis presented in this work is an efficient mean for structural engineers to identify critical locations of overhead structure and facilitate asset managers to prioritize inspection and maintenance works for deteriorated overhead structures.

List of symbols

β	Reliability index
t_{wu}	Remaining thickness of upper web
t_{wb}	Remaining thickness of bottom web
h_{wu}	Height of upper web
h_{wb}	Height of bottom web
T_{fu}	Remaining thickness of upper flange
T_{fb}	The remaining thickness of bottom flange
w_f	Width of the flange
Z_e	Effective section modulus
Z_x	Elastic modulus of I section steel in the x axis (strong axis)
S_x	Plastic modulus of I section steel in the x axis (strong axis)
y_e	Position of elastic axis of I section steel
y_p	Position of plastic axis of I section steel
M_s	Sectional moment strength of I section steel
N_s	Sectional compressive strength of I section steel
V_w	Shearing strength of I section steel
p_w	Wind pressure of unit length on the overhead wires
p_s	Wind pressure of unit are on the overhead structure
$d(t)$	Time-dependent thickness of corrosion product
R	Resistance in limit state function
S	Load effect in limit state function
F_y	Yield stress of steel
A, B	Environmental parameters
t	Elapsed time
V_{des}	Design wind speed
ρ_{air}	Density of air
C_d	Drag coefficient
C_{fig}	Dynamic response factor
C_{dyn}	Aerodynamic factor

✉ Ricky W. K. Chan, ricky.chan@rmit.edu.au | [1]Department of Transport, Melbourne, VIC, Australia. [2]School of Engineering, RMIT University, Melbourne, VIC, Australia.

1 Introduction

Overhead structures play a vital role in the operation of electrified rail networks. They support overhead electrical wires along the track that provide electrical power to the operation of trains. In China, the millage of electric railway track exceeds 48,000 km [1]. The spacing of overhead structures depends on track geometry, in straight tracks typical the spacing is between 50 and 70 m. The amount of overhead structures in one country is in the order of millions. They support high-voltage (from 750 V to 25 kV) wirings through catenary wire systems [2]. Overhead structures are constructed in several common structural forms depending on the number of tracks: portals, trusses, single masts, and cantilevers, etc. The structural components of overhead structures may include masts (i.e. columns), bridges (i.e. beams) and the non-structural components comprise catenary wires, contact wires, pull-off arms, cantilever arms insulators and fasteners, etc. A portal overhead structure is shown in Fig. 1. In Australia, electrification of metropolitan railway began in late 1910s, the first generation of overhead structures are riveted lattice structures were standing in the atmosphere with some kind of simple means of corrosion protection (i.e. paint coatings), which induced the old overhead structures to be very vulnerable to corrosion damage.

Unlike buildings, overhead structures are simple steel structures that lack redundancies and failure in a single location such as mast-bridge connection may cause excessive deflection or even complete collapse. A failed overhead structure may cause injuries or fatalities via

electrification. In less severe circumstances it may suspend the operation train service and cause delays to the commuters and indirectly causing economic loss. These steel structures are exposed to the environment and gradual deterioration of steel due to corrosion jeopardises their strengths and serviceability. Structural assessments of overhead structures and typically carried out manually by experienced inspectors at predetermined intervals. Maintenance is carried out when structural damages are noticeable, typically through visual inspection. Whilst this method of inspection and maintenance is globally proven to be reliable based on past-experience, the process is labour-intensive, and maintenance often requires suspension of train service. It is also reliance on sufficient and relevantly skilled inspectors being available to visit assets. Human errors in the performance and analysis of inspection outcomes are potential risks. Difficult access, for example structural components at great height, concealed components, proximity to high voltage transmission lines are examples of addition complexities in traditional in-person inspections. It is imperative to develop a more accurate way to predict the failure location and prioritise inspections and maintenance works. Overhead structures are typically designed according to local steel design standards, supplemented by technical information such as weight of wirings particular to train companies. A universally accepted design standard is not available. Uncertainties related to materials, geometric properties, loading and environmental conditions play a significant role in the long-term performance of the infrastructure. Thus, structural reliability analysis which allows these uncertainties are chosen as the methodology to evaluate the probability of failure of individual structural components of a portal overhead structures. Many asset owners now adopt a scientific way of making decisions. A reliability approach allows them to make decisions based on minimization of costs and/or minimization of committed resource usage subject to given reliability requirements of the structures.

Despite the large quantity and importance of overhead structures in modern transportation networks, research into their reliability is rare in literature. The objective of this study is to develop a reliability-based method for the assessment of railway overhead wiring structures. Due to the fact that majority of these overhead wiring structures are exposed to the environment, and the horizontally positioned I-section tend to accumulate moisture and accelerate corrosion on their bottom flanges and lower parts of the webs, the proposed method provides a more precise model to describe the reduced capacity due to corrosion. In this investigation, limit state functions are formulated based on the load effects and structural capacity as described in the Australian Standards [3, 4] and technical guides on overhead structures [5].

Fig. 1 Portal type overhead wiring structure

In the structural resistance modelling, a new deterioration model for steel wide-flange sections is presented. Structural reliability analysis is conducted using the well-known first order reliability method (FORM). A worked example on a portal overhead structure is illustrated with its structural performance quantified to obtain the time-dependent reliability index, β. The method presented in this article may become a more accurate and efficient means for asset owners to make reliability-based decisions, such as optimising the time frame to perform structural assessments, maintenance and/or decommissioning. The method presented in this article also assists structural engineers to locate the critical structural components or corrosion-affected overhead wiring structure.

2 Theoretical bases and related methods

2.1 Structural reliability analysis

Structural reliability analysis begins with a limit state function in terms of a number of basic random variables [6]. A basic structural reliability only take account one load effect S resisted by one resistance R [7]. The limit state function in structural reliability is written as:

$$g(X) = R - S \tag{1}$$

A positive $g(X)$ (i.e. $R > S$) indicates the structure or the element remain in the safe domain; whereas a negative value indicates failure domain. The probability of structural failure can be determined by Eqs. (2) and (3):

$$p_f = P[g(X) < 0] \tag{2}$$

$$p_f = \int_{g(X)} p_x(X)dx \tag{3}$$

The first order reliability method (FORM) approximates the limit state function $g(X)$ at design point x^* by using the first order Taylor's expansion (Eq. 4), which simplifies the calculation of probability of failure (see Eq. 5) [7, 8]. The result of such reliability calculation can be expressed by reliability index, β which is the mean value of limit state function divided by the standard deviation of limit state function (Eq. 6). Also, the reliability index β can be geometrically understood as the minimum distance between the limit state criterion expressed as a surface $g(X_1, X_2, \ldots, X_n) = 0$ in the space of standardised coordinate and its coordinate origin.

$$Z \approx Z_L = g_x(x^*) + \sum_{i=1}^{n} \frac{\partial g_x(x^*)}{\partial X_i}\left(\mu_{X_i - x_i^*}\right) \tag{4}$$

$\frac{\partial g_x(x^*)}{\partial X_i}$ is the gradient vector evaluated at the expansion point x^*

$$p_f = \Phi(-\beta) \tag{5}$$

where $\Phi()$ is the standard normal distribution function.

$$\beta = \frac{\mu_z}{\sigma_z} \tag{6}$$

Using Eqs. (7) and (8), the mean value μ_{ZL} of the linearized limit state function Z_L can be expressed as Eq. 9.

$$E(Z) = \mu_z = \sum_{i=1}^{n} a_i E(X_i) = \sum_{i=1}^{n} a_i \mu_{Xi} \tag{7}$$

$$
\begin{aligned}
E\left[(Z - \mu_z)^2\right] &= var(Z) = \sigma_z^2 \\
&= \sum_{i=1}^{n} a_i^2 var(X_i) + \sum_{j \neq 1}^{n} \sum_{i=1}^{n} a_i a_j cov(X_i, X_j)
\end{aligned} \tag{8}
$$

$$\mu_{Z_L} = g_x(x^*) + \sum_{i=1}^{n} \frac{\partial g_x(x^*)}{\partial X_i}\left(\mu_{X_i - x_i^*}\right) \tag{9}$$

and the standard deviation σ_{ZL} of the linearized limit state function Z_L can be express as follow:

$$\sigma_{Z_L} = \sqrt{\sum_{i=1}^{n}\left(\frac{\partial g_x(x^*)}{\partial X_i}\right)^2 \sigma_{X_i}^2} \tag{10}$$

Equations (9) and (10) can be applied to Eq. (6), and the reliability index is obtained as follow [7]:

$$\beta = \frac{\mu_{Z_L}}{\sigma_{Z_L}} = \frac{g_x(x^*) + \sum_{i=1}^{n} \frac{\partial g_x(x^*)}{\partial X_i}\left(\mu_{X_i - x_i^*}\right)}{\sqrt{\sum_{i=1}^{n}\left(\frac{\partial g_x(x^*)}{\partial X_i}\right)^2 \sigma_{X_i}^2}} \tag{11}$$

However, in the case that variables $\boldsymbol{X}$ consist of the non-normally distributed variables X_i, these variables need to be transformed to their normalised form using following functions [9]:

$$\mu_{X_i'} = x_i^* - \Phi^{-1}\left[F_{X_i}(x_i^*)\right]\sigma_{X_i'} \tag{12}$$

$$\sigma_{X_i'} = \frac{\varphi\left(\Phi^{-1}\left[F_{X_i}(x_i^*)\right]\right)}{f_{X_i}(x_i^*)} \tag{13}$$

where $F_{Xi}(x_i^*)$ is the cumulative distribution function of the non-normal distribution, $f_{Xi}(x_i^*)$ is the probability density function of the non-normal distribution, $\varphi()$ is the standard normal density function.

Different asset owners, based on their specific requirements such as costs of inspections, maintenance, downtime costs, failure and replacement costs and compensation costs, etc. will adopt a different target probability of failure p_{ft}. In Australia, the Australian Standard AS5104 General Principles on Reliability for Structures provides a comprehensive principles of reliability decision making. Tentative values of minimum target reliabilities based on Life Quality Index (LQI) acceptance criterion are provided in the standard, for example the LQI target reliability $\beta = 3.7$ ($p_f = 10^{-4}$) for "medium lifesaving costs". A more comprehensive descriptions and list of target reliability can be found in the standard. Specific values are not enforced by the standard.

2.2 Corrosion model for structural steel sections

Strength of structural steel deteriorates over time as a result of corrosion. Engineers and researchers have identified five main forms of corrosion, namely (1) general surface corrosion, (2) pitting corrosion, (3) crevice corrosion, (4) galvanic corrosion and (5) stress crack corrosion. Among these forms, the most common form is general surface corrosion in which rust is uniformly distributed over the entire exposed surface [10]. In this study, deterioration of steel is assumed to be general surface corrosion. Corrosion rates of steel from various outdoor environments (i.e. rural, urban and marine environment) were extensively studied [11, 12]. A power function has been proposed:

$$d(t) = At^B \tag{14}$$

where $d(t)$ is corrosion wastage depth (in µm) after t number of years of exposure. A is the initial corrosion loss (i.e. the corrosion penetration after the first year of exposure). B is the corrosion rate under the long-term exposure. Parameters A and B are typically determined by regression analysis of the measured data., Although other corrosion models are available, this power corrosion rate function is simple and thus most commonly used in literatures [11, 13]. Derived from 8 years of atmospheric corrosion tests of weathering steel and carbon steel under different exposure environment, suggested values of parameters A and B are given in Table 1 [12].

Table 1 Parameters of corrosion model for Eq. (14) [10, 12]

Rural environment	A	B
Mean value, μ (unit: µm)	34	0.65
Coefficient variation σ/μ	0.09	0.1

2.3 Validation of corrosion model

To validate the corrosion model parameters of Eq. (14) and Table 1, samples were collected from a dismantled overhead wiring structure located in South-eastern Australia. The exact age of the steel structure cannot be determined, however, from its drawing archive it was dated 1910, which agreed with the historical development of railway electrification of the region. To determine the thickness loss, ultrasonic thickness measurement was conducted to Australian Standard 1710. The original sample was cut into a rectangular shape with a bandsaw, as shown in Fig. 2a. To obtain meaningful readings, the surface rusts had to be removed, as shown in Fig. 2b. Twelve measurements were made on each sample in a regular grid manner, as shown in Fig. 2c. The results are summarized in Table 2. The original thicknesses were obtained from the drawing archive. Results have demonstrated that an average of 0.838 mm was lost in approximately 100 years, while the Corrosion Model presented in Eq. 14 using parameters
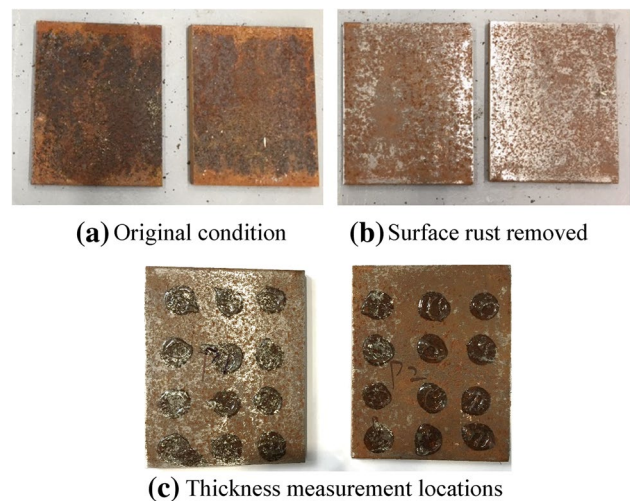

(a) Original condition   **(b)** Surface rust removed

(c) Thickness measurement locations

Fig. 2 Samples collected from overhead wiring structures (sample P1 and P2 shown)

Table 2 Thickness loss of the structural steel after the exposure in the environment

Sample ID	Nominal original thickness (mm)	Mean measured thickness (mm)	SD (mm)	Mean thickness loss (mm)
P1	7.94	7.79	0.08	0.15
P2	7.94	7.51	0.14	0.43
C1	9.14	8.43	0.56	0.71
A1	10.92	9.41	0.31	1.51
A2	10.92	9.53	0.08	1.39
			Average	0.838

for rural environment gives 0.503–0.915 mm (using $B \pm \sigma$). Thus, the corrosion model gives reasonable approximation to the observed thickness loss.

3 Proposed modified corrosion decay model

The formation of iron oxide reduces the effective thickness of steel elements and compromises the strength of steel sections. Gradually thinning of steel members, if not repair or replace will eventually cause structural failure. To account for the section loss due to corrosion, it is typical to assume thickness is reduced uniformly as a function of time. However, when an I-section is positioned horizontally, in an exposed condition moisture tends to accumulate on the bottom flange and accelerate corrosion in the lower region of section [10]. This phenomenon is common in overhead wiring structures as they are typically exposed in the atmosphere. Figure 3 shows a typical exposed I-section of an overhead wiring structure in a busy train station. Signs of corrosion to the bottom part of the web and bottom flange are clear, as indicated by brown colour change.
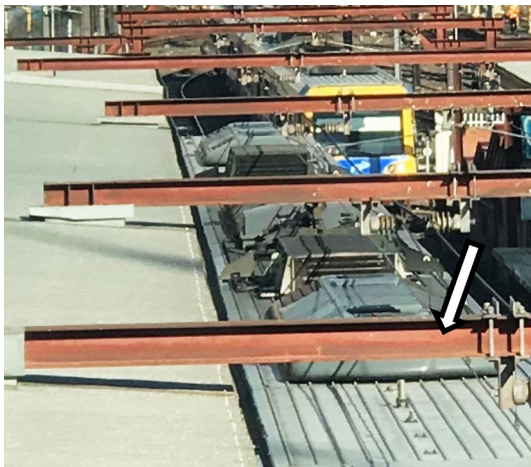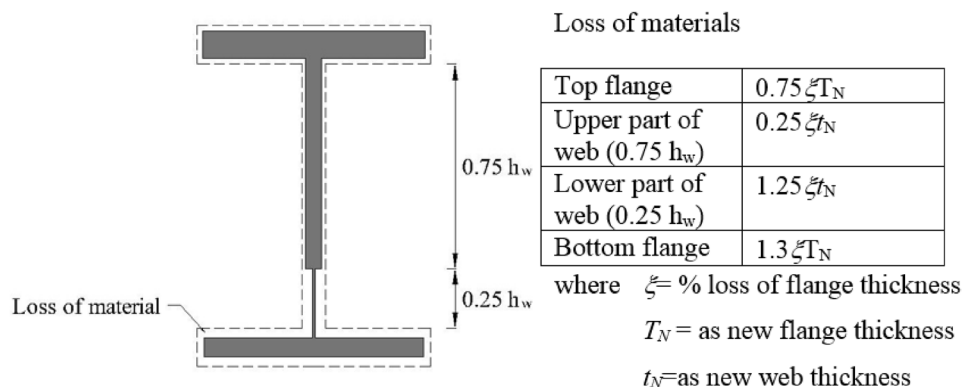

Fig. 3 Corrosion pattern on an exposed I-section

To address this phenomenon, a corrosion decay model which splits the section into four regions was proposed by Kayser [10]. Different loss of materials is assigned to top flange, upper part of web (75% height of the web), bottom part of the web (25% height of the web) and the bottom flange respectively, as shown in Fig. 4. The model was established based on the experimental thickness measurement of four I-sections that had been used for over 30 years. The experimental results given in Table 3 are extracted from literature [14].

A Modified Corrosion Decay Model (MCDM) is proposed herein. Based on the review of published data in [14] on horizontally positioned I-sections, coefficients is determined from normalizing the averaged thickness loss to that of top flange. For example, the averaged loss on top flange was 2.62 mm and that of bottom flange was 4.22 mm. The coefficient for bottom flange is therefore 4.22 mm/2.62 mm = 1.61. Other coefficients are listed in Fig. 5. In the "Varying Thickness Loss Corrosion Decay Model" proposed by Sarveswaran et al. [14], a ξ factor is used which is the percentage loss of flange thickness (see Fig. 4). Instead, in this research the corrosion rate is assumed independent of the original steel thickness. As a result, two corrosion acceleration factors α and γ are introduced here for the flanges and web respectively. In addition, the power function (Eq. 14) is applied to MCDM to describe the thickness loss over time. The new reduction factors and the proposed MCDM is illustrated in Fig. 5.

4 Application of modified corrosion decay model to overhead structures

4.1 Modelling load effects

Overhead structures are generally designed for four types of loadings: (1) dead loads, (2) radial load, (3) wind loads on wires and (4) wind loads on structure [5]. Dead load includes the self-weight of structural elements and the non-structural elements (cantilever arms, overhead wires,

Fig. 4 Corrosion decay model with varying thickness loss [15]

Loss of materials

Top flange	$0.75 \xi T_N$
Upper part of web ($0.75\ h_w$)	$0.25 \xi t_N$
Lower part of web ($0.25\ h_w$)	$1.25 \xi t_N$
Bottom flange	$1.3 \xi T_N$

where ξ = % loss of flange thickness

T_N = as new flange thickness

t_N = as new web thickness

Table 3 Thickness loss due to corrosion (mm) [14]

	μ	c_v
Top flange		
As new thickness (mm)	10.2	–
Measured thickness (mm)	7.58	0.03
Loss (mm)	2.62	0.10
% reduction	25.7	0.10
Bottom flange		
As new thickness (mm)	10.2	–
Measured thickness (mm)	5.98	0.17
Loss (mm)	4.22	0.24
% reduction	41.4	0.24
Upper web		
As new thickness (mm)	6.10	–
Measured thickness (mm)	5.67	0.032
Loss (mm)	0.44	0.33
% reduction	7.2	0.33
Lower web		
As new thickness (mm)	6.10	–
Measured thickness (mm)	3.85	0.18
Loss (mm)	2.25	0.27
% reduction	36.9	0.27

Position	Corrosion product thickness
Top flange	$\alpha d(t)$
Bottom flange	$1.61\,\alpha d(t)$
Upper web ($0.75 h_w$)	$0.17\gamma d(t)$
Lower web ($0.25 h_w$)	$0.86\gamma d(t)$

$d(t) = At^B$

α is the corrosion acceleration factor for flange.
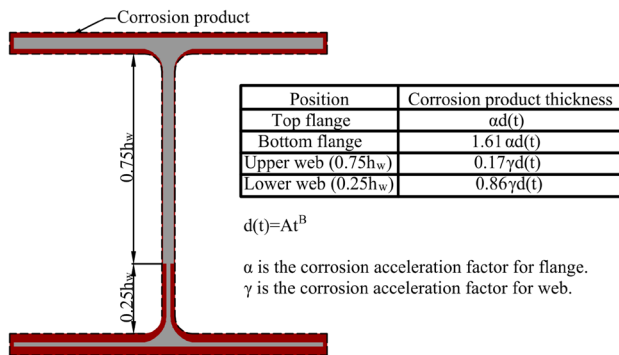γ is the corrosion acceleration factor for web.

Fig. 5 Modified corrosion decay model

insulators, etc.). The self-weight of the structural elements is treated as uniformly distributed loads. The self-weight of the non-structural elements is considered as the point loads. Dead loads are assumed to be normally distributed variables. Radial loads are produced by the directional changes and tension effects of overhead wires. Their directions are assumed horizontal. The value of the load depends on the degree of directional change and tension in the wire. The radial load is modelled as point loads to the drop vertical. Radial loads are assumed to be lognormal distributed variables. The wind generates loading over the entire overhead wiring which can span up to 70 m, and also directly on the structural elements. Therefore, the wind load is divided as two components: (1) wind load

on overhead wires; (2) wind load on structural members. The wind load on the overhead wires (P_{ww}) is modelled as point loads imposed on the drop vertical. It is determined by Eq. (15),

$$P_{ww} = p_w L_{ws} \tag{15}$$

p_w is the wind pressure per unit length and L_{ws} is the wind span of the wires. The direction of P_{ww} is assumed to remain horizontal and towards the same direction as in radial load to produce the worst combination. According to the industry standard and Australian Standard [3–5, 16], the wind pressure, p_w exerted on overhead wires, in Pascal, is expressed as below:

$$p_w = 0.613 (V_{des})^2 C_d \tag{16}$$

where V_{des} is the design wind speed, C_d is the drag coefficient (0.8 for the contact wire and 1.03 for the catenary wire). On the other hand, the wind loads on structural members p_s are assumed distributed uniformly on the surface of the structure. The directions of p_s consist of in-plane and out-of-plane of overhead structures, and 45° to the track. According to the Australian Standard [3–5, 16], p_s, in Pascal, is expressed as below:

$$p_s = (0.5\rho_{air})(V_{des})^2 C_{fig} C_{dyn} \tag{17}$$

ρ_{air} is density of air, which is taken as 1.2 kg/m³, C_{fig} is aerodynamic factor and C_{dyn} is the dynamic response factor.

4.2 Modelling resistance

The failure modes of overhead structures may consist of the failures in of shear and flexure strength of the structural members, compression buckling, combined compression and bending and strength of the structural connections. The resistance of each mode follow the strength capacity formulas in the Australian Standard AS 4100 [3]. To model the time-dependent reduction in capacity, yield moment model for steel structural connection, corrosion decay model [14, 15] and corrosion rate power model [11, 12].

4.2.1 Capacities of structural members

The nominal section in-plane moment strength M_s for a beam is formulated as Eq. 6 based on Eq. (18) from Australian Standard AS 4100 [3].

$$M_s = Z_e f_y \tag{18}$$

where Z_e is effective section modulus which is determined by the minimum value of *1.5Z* (elastic section modulus) or S (plastic section modulus); f_y is the yield strength of the

section material. However, the bridge is under the exposure of the environmental corrosion, the section properties are changing over time according to the remaining thickness of web and flange. MCDM is applied to calculate the time-dependent effective section modulus and is express as followings:

$$Z_x = \left[\frac{(T_{fu}^3 w_f) + (T_{fb}^3 w_f) + (h_{wu}^3 t_{wu}) + (h_{wb}^3 t_{wb})}{12} \right.$$
$$+ (T_{fb} w_f)\left(\frac{T_{fb}}{2} - y_e\right)^2 + (T_{fu} w_f) \times \left(\frac{T_{fu}}{2} + T_{fb} + h_w - y_e\right)^2$$
$$\left. + (h_{wu} t_{wu})\left(\frac{h_{wu}}{2} + T_{fb} + h_{wb} - y_e\right)^2 + (h_{wb} t_{wb})\left(\frac{h_{wb}}{2} + T_{fb} - y_e\right)^2 \right] \div y_e$$
$$(19)$$

$$y_e = \left[(T_{fu} w_f)\left(\frac{T_{fu}}{2} + h_w + T_{fb}\right) + (T_{fb} w_f)\frac{T_{fb}}{2} \right.$$
$$\left. + (t_{wu} h_{wu})\left(\frac{h_{wu}}{2} + h_{wb} + T_{fb}\right) + (t_{wb} h_{wb})\left(\frac{h_{wb}}{2} + T_{fb}\right) \right] \div Area$$
$$(20)$$

$$Area = (T_{fu} w_f) + (T_{fb} w_f) + (t_{wu} h_{wu}) + (t_{wb} h_{wb}) \quad (21)$$

$$S_x = (T_{nu} w_f)\left|y_p - \frac{T_{nu}}{2}\right| + (T_{nb} w_f)\left|h_w - (y_p - T_{nu}) + \frac{T_{nb}}{2}\right|$$
$$+ [t_{wu}(y_p - T_{nu})] \times \left|y_p - \frac{y_p - T_{nu}}{2}\right| + \left[\frac{t_{wu}(h_{wu} - (y_p - T_{nu}))^2}{2}\right]$$
$$+ (t_{wb} h_{wb}) \times \left|(h_{wu} - (y_p - T_{nu})\right| + (T_{nb} w_f)\left|h_w - (y_p - T_{nu}) + \frac{T_{nb}}{2}\right|$$
$$(22)$$

$$y_p = \left[\frac{T_{nb} w_f + t_{wb} h_{wb} + (h_{wu} + T_{nu}) t_{wu} - T_{nu} w_f + T_{nu} t_{wu}}{2 t_{wu}} \right]$$
$$(23)$$

The nominal section shear strength V_w for the web from beams is formulated as following:

$$V_w = 0.6 f_y A_w \quad (24)$$

A_w is the gross sectional area of the web, f_y is the yield stress of material. Based on the MCDM, the time-dependent area is expressed as below,

$$A_w = (t_{wu} h_{wu}) + (t_{wb} h_{wb}) \quad (25)$$

Axial compression squash strength, N_s, is determined by,

$$N_S = k_f f_y A_n \quad (26)$$

k_f is the form factor and is, A_n is the net area cross-sectional area neglecting any penetrations. The moment strength of mast under combination of axial compression and bending moment is expressed as below:

$$M_r = M_s\left(1 - \frac{N^*}{\phi N_S}\right) \quad (27)$$

N^* is the design axial force, N_s is the nominal section axial load capacity, M_s is the nominal section moment capacity, ϕ is the capacity factor.

4.3 Time-dependent yield moment strength for structural connection

Rotational stiffness and strength of moment-resisting connections depends on structural details such as number and positions of bolts, presence of web-stiffeners, and size and grades of welds. Based on yield-line theory, the authors recently proposed an expression for time-dependent strength of structural connection [17]:

$$M_y = \sum_{n=1}^{N} \frac{f_y(T - At^B)^2}{4} \Theta_n L_n \bigg/ \theta_e \quad (28)$$

where f_y is the yield stress of base plate, T is the original thickness of the endplates, θ_n is the plastic rotation at the nth yield line, L_n is the length of the nth yield line, θ_e is the virtual rotation induced by the moment M_y.

5 Worked example

Portal type overhead structures with masts and bridges fabricated from universal column sections have been extensively used since 1975 in Australia [5]. A railway portal overhead structure (see Fig. 6a) is selected as a worked example for assessment. The selected structures consisted of two masts, one bridge and a drop vertical which is attach to the mid length of the bridge. The two masts are connected to the both ends of the bridge via flushed endplate connections. The bases of masts are welded on baseplates connected to an embedded concrete foundation via anchored holding bolts.

The value of applied load on overhead structures is chosen based on the design standard [5]. The dead loads of the components of the selected overhead structures are listed in Table 4. The radial load imposed on the structure is listed in Table 5. It is assumed that the direction of the wind force is 45° to the tracks. The wind load on wires is assumed at 45° to the tracks (WW45) and it is divided into in-plane wind force and out-of-plane wind force. Wind loads on wire and overhead wiring structures are listed in Tables 6 and 7 respectively. Based on the design standard [5], load combination is determined by Eq. (29),

$$LC = 1.2DL + 1.2RL + WW + WS \quad (29)$$

The flushed endplate bridge-mast connection and pinned column bases are modelled as rotational springs (see Fig. 6b) [17]. The resultant bending moment, axial force and shear force diagrams are determined by a
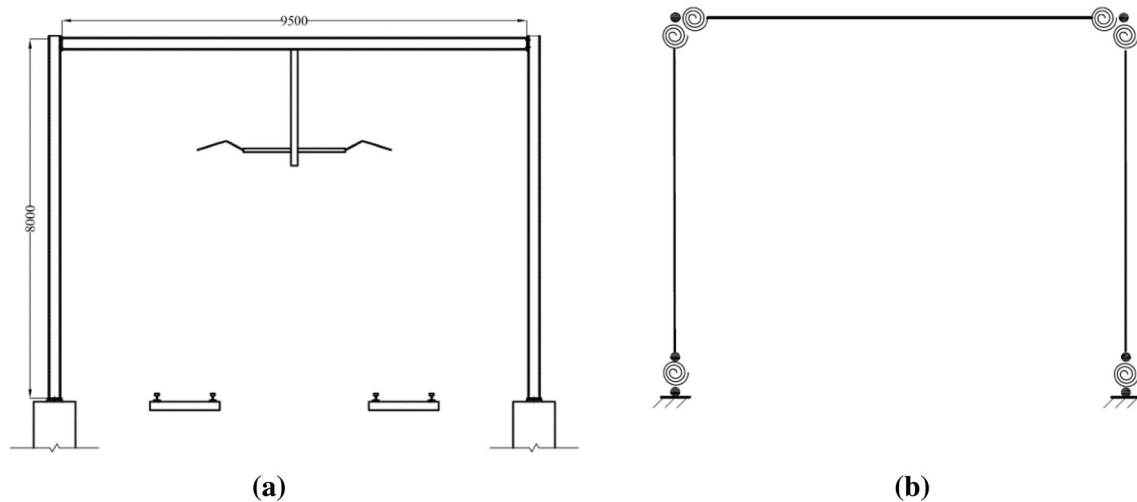
Fig. 6 **a** Selected portal overhead structure for example, **b** structural model

Table 4 Dead load (DL) (unit: kN, all random variables have normal distribution)

Component	μ	c_v	References
Bridge	8.51	0.093	[19]
Mast	7.16	0.093	[19]
Electrical fitting	0.75	0.093	[5]
Drop vertical	0.93	0.093	[19]
Wires	2.42	0.093	[5]

Table 5 Radial load (RL) (Unit: kN, All Random Variables have Lognormal Distribution)

Parameters	μ (kN)	c_v	References
Radial load for catenary wire	1.9	0.18	[5]
Radial load for contact wire	1.6	0.18	[5]

Table 6 Wind load on wire (WW) (Unit: kN, all random variables have lognormal distribution)

Parameters	μ (kN)	c_v	References
Wind load on contact wire	0.81	0.18	[1]
Wind load on catenary wire	1.21	0.18	[4]

non-linear three-dimensional model from SpaceGass [18] and the results are shown in Fig. 7a–d.

The resistance models are based on the formulated functions in the previous section. The statistical values in the resistance models are listed in Table 8. The thickness parameters are assumed normal distributed and the yield stress parameter is assumed lognormal distributed.

Rural environment (parameters listed in Table 1) is selected for the determination of structural deterioration according to Eq. 14. For the structural resistance of the horizontally positioned bridge, the MCDM described in Sect. 3 is applied. α and γ is assumed to be 2.54 and 1.31 respectively. Figure 8 shows the deterioration of the normalised time-dependent structural strength of different structural components. A comparison is made in the Fig. 8 of calculating bridge bending strength using the original corrosion decay model. It can be observed that under the proposed MCDM, loss of strength is more rapid.

Based on the listed load effect model and resistance model, a reliability analysis is conducted in accordance with FORM. According to the structural analysis as shown in Fig. 7, the most critical load effects are chosen for the reliability analysis on each structural component. The time-dependent reliability index for the structural components are determined and shown in Fig. 9. From the results, bridge-mast connection has the lowest reliability over time, while the bridge bending strength experienced the most rapid decline over time. On the contrary, the mast shearing strength and compression strength are the most reliable components. The results presented in this example indicate to the asset owners that more frequent inspections and assessments shall be made to the bridges and their connections.

6 Conclusion

Overhead wiring structures are vital components in any electrified railway network. They are typically lightweight and simple steel structures which lack redundancy. They are usually constructed as simple portal

Table 7 Wind load on overhead wiring structure (WS) (unit: kN/m, all random variables have lognormal distribution)

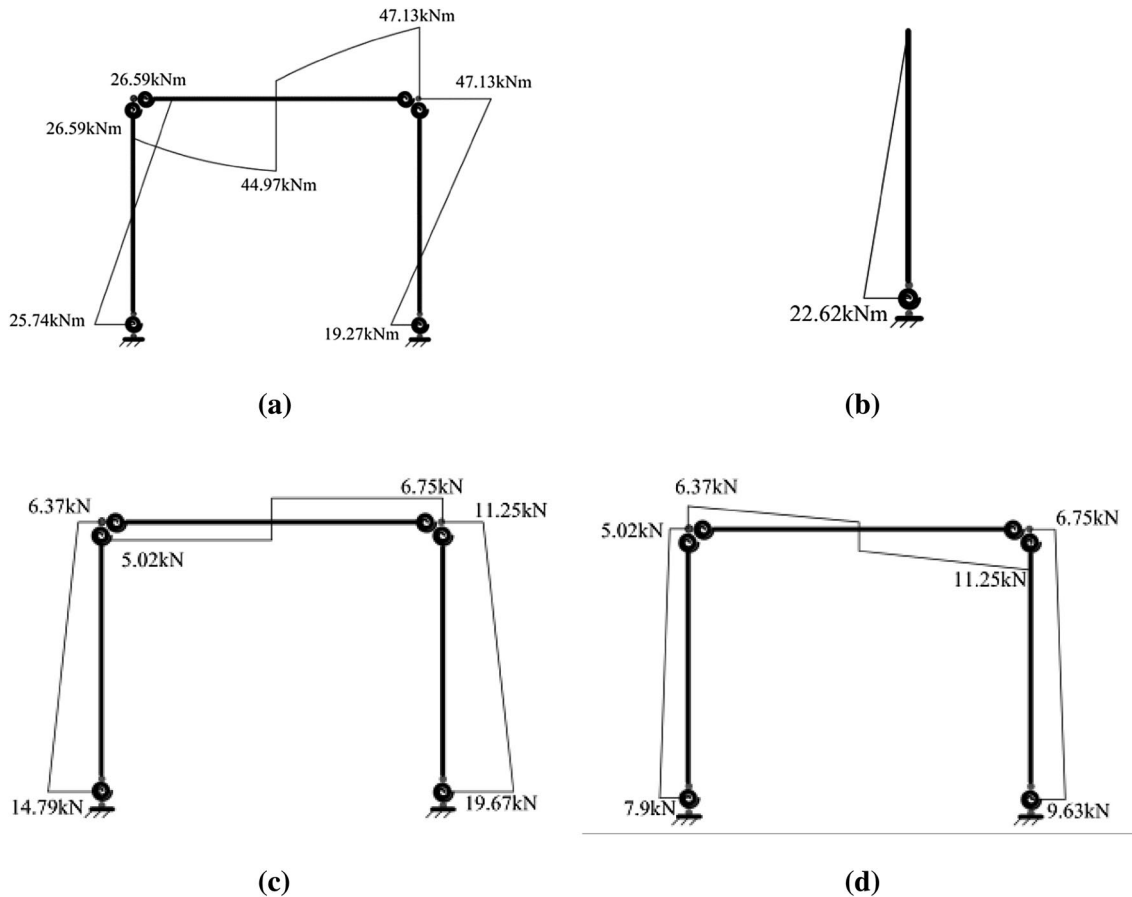| Parameters	μ	c_v	References
Wind load on mast (horizontal in-plane)	0.36	0.18	[1]
Wind load on bridge (horizontal in-plane)	0.008	0.18	[5]
Wind load on drop vertical (horizontal in-plane)	0.22	0.18	[5]
Wind load on mast (horizontal out-of-plane)	0.36	0.18	[5]
Wind load on bridge (horizontal out-of-plane)	0.016	0.18	[5]
Wind load on drop vertical (horizontal out-of-plane)	0.22	0.18	[5]

Fig. 7 **a** In-plane bending moment diagram, **b** out-of- plane bending moment diagram, **c** shear force diagram and **d** axial force diagram

Table 8 Statistical parameters in resistance models

Parameters	μ	c_v	References
f_y	300 MPa	0.1	[17]
T_{fl}	17.3 mm	0.013	[17]
T_{bp}	32 mm	0.013	[20]

frames or fix-based cantilevers. Failure at a single location within a structure may jeopardize the structural integrity and collapse of such simple structures may

cause significant impact such as suspension of train service or even train derailment. Overhead structures are exposed to the atmosphere and deterioration due to corrosion represents durability issues. This article presents a time-dependent reliability analysis with the following features:

1. A power function corrosion model is adopted to depicts reduction of steel thicknesses over time. The model parameters are validated by thickness measurements of 100-year old samples of overhead wiring structures;
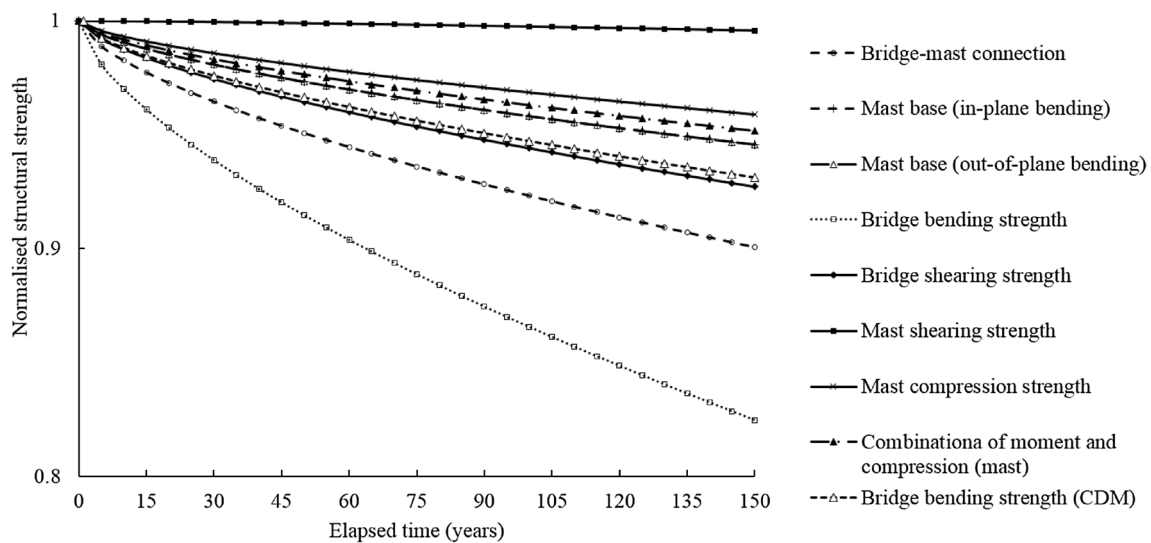
Fig. 8 Time-dependent structural strength for various structural components
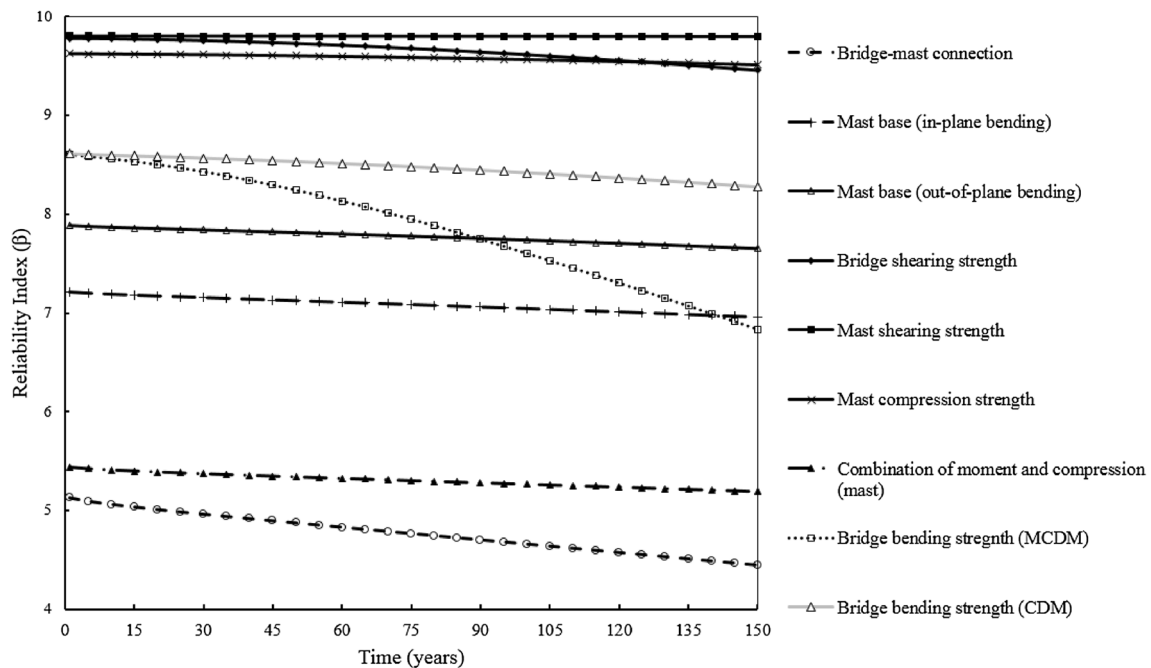

Fig. 9 Time dependent reliability index of various structural components

2. A modified corrosion decay model is proposed to describe the reduction in strengths of wide-flange steel sections in exposed condition. This model applies to horizontally positioned I-beams which are exposed to the environments. It captures the non-uniform thickness loss due to moisture accumulation in the bottom half of section.

3. A reliability analysis using the proposed modified corrosion decay model is demonstrated in worked example of a portal-type overhead wiring structure. It is found that the rotational strength of bridge-mast connection and the bending strength of the bridge at the attachment point to drop vertical are the most structural components with the least reliability indices.

4. The bridge bending strength shows the most rapid decline in reliability index.

It is concluded that the reliability-based time-dependent assessment method can be used a rational method to locate the critical structural components of the overhead structures. It also facilitates assets owners to make reliability-based decisions, such as scheduling structural inspections and repair works based on accepted target reliabilities.

Compliance with ethical standards

Conflict of interest On behalf of all authors, the corresponding author states that there is no conflict of interest.

References

1. Chen Z (2012) China's electric railway mileage exceeds 48,000 km, in Xinhua
2. LLP A.B.A. (2015) Network rail guide to overhead electrification 132787-ALB-GUN-EOH-000001. London, UK
3. Australia Standards (1998) AS 4100-1998 steel structures, in Sydney: Standards Australia
4. Joint Technical Committee (2011) AS/NZS 1170.2: 2011 structural design actions—part 2: wind actions. Australian/New Zealand Standard (AS/NZS): Joint Technical Committee BD-006, Australia/New Zealand
5. New South Wales Railcorp (2011) Design of Overhead Wiring Structures and Signal Gantries, Engineering Manual TMC311
6. Thoft-Christensen P, Baker MJ (1982) Structural reliability theory and its applications. Springer, Berlin
7. Melchers RE (1999) Structural reliability analysis and prediction. Wiley, New York
8. Hasofer AM, Lind NC (1974) Exact and invariant second-moment code format (for reliability analysis in multivariate problems). Am Soc Civ Eng Eng Mech Div J 100:111–121
9. Rackwitz R, Flessler B (1978) Structural reliability under combined random load sequences. Comput Struct 9(5):489–494
10. Kayser JR (1988) The effects of corrosion on the reliability of steel girder bridges. Dissertation Abstracts International
11. Townsend H, Zoccola J (1982) Eight-year atmospheric corrosion performance of weathering steel in industrial, rural, and marine environments. Atmospheric Corrosion of Metals, ASTM STP, vol 767, pp 45–59
12. Albrecht P, Naeemi AH (1984) Performance of weathering steel in bridges. NCHRP report, 272
13. Akgül F, Frangopol DM (2004) Lifetime performance analysis of existing steel girder bridge superstructures. J Struct Eng 130(12):1875–1888
14. Sarveswaran V, Smith J, Blockley D (1998) Reliability of corrosion-damaged steel structures using interval probability theory. Struct Saf 20(3):237–255
15. Rahgozar R (2009) Remaining capacity assessment of corrosion damaged beams using minimum curves. J Constr Steel Res 65(2):299–307
16. Ausgrid, NS220 overhead design manual (2015)
17. Hu B, Chan R (2016) Time-dependent yield moment model for deteriorated steel connections. In: International conference on architectural engineering and civil engineering, Shanghai, China
18. Gass S (2014) Documentation for the SPACE GASS structural engineering design and analysis software
19. AS/NZS 3679.1:2016 Structural steel - Hot-rolled bars and sections
20. Hu B, Chan R, Li CQ (2016) Remaining capacity assessment of corrosion damaged column bases. In: 4th international conference on sustainability construction materials and technologies, Las Vegas, USA

Publisher's Note Springer Nature remains neutral with regard to jurisdictional claims in published maps and institutional affiliations.